Acta Cryst. (1961). **14**, 1097

A diffusionless UC_2 (cubic) to UC_2 (Tetragonal) Transformation.*

By Roger Chang, *Atomics International, A Division of North American Aviation, Inc., Canoga Park, California, U.S.A.*

(*Received* 10 *April* 1961 *and in revised form* 15 *May* 1961)

A diffusionless phase transformation between MX_2 (cubic CaF_2 structure) and MX_2 (tetragonal structure) has been reported by Yakel (1958) and by Chang (1960) for TiH_2 and ZrH_2. The transformation is characterized by co-operative atom movements involving a pure lattice distortion combined with a twinning shear (over a fraction of the crystal) which does not affect the lattice structure but produces a macroscopic change in shape.

This note describes the characteristic features of another diffusionless transformation for UC_2. The transformation from the high-temperature UC_2 phase ('CaF_2' structure,† $a_0 \cong 5{\cdot}41$ Å at 1820 °C.) to a tetragonal phase (CaC_2 structure, $a \cong 3{\cdot}68$, $c \cong 5{\cdot}88$ Å at 1820 °C.) takes place at 1820 to 1830 °C. (Wilson, 1960), the low-temperature tetragonal phase being composed of twins. Our microstructural studies reveal the following orientation relation-ships between the two phases:

Planes:	(001) cubic parallel to (001) tetragonal
Directions:	[011] cubic parallel to [111] tetragonal

within an experimental error of $\pm 1°$. Both the habit plane and twinning plane indices cannot be determined with confidence but are believed to correspond to the (101) type planes of the cubic phase.

The requirement of a macroscopic shear for the UC_2 transformation is obvious from the grain-boundary offset shown in Fig. 1 (Chubb & Phillips). The magnitude of macroscopic shear, estimated from the distortion of a straight graphite inclusion across neighboring twins shown in Fig. 2, is about 0·07 to 0·10, corresponding to a shear angle of 4 to 6°.

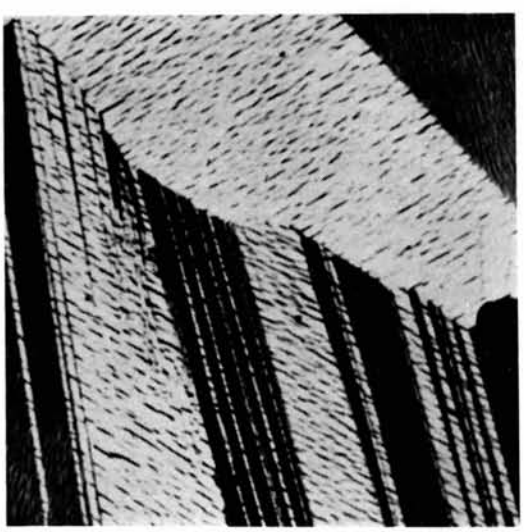

Fig. 1. Uranium—8·5 weight per cent carbon alloy showing grain-boundary offset (1000×).

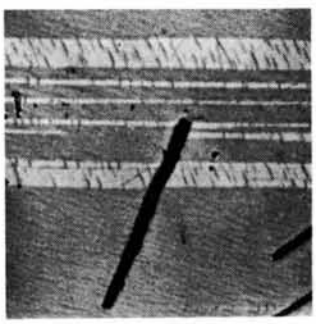

Fig. 2. Uranium—9·0 weight per cent carbon alloy showing distortion of a straight graphite inclusion across neighboring twins (1500×).

The experimental observations are in agreement with predictions of the phenomenological theories of Wechsler–Lieberman–Read (1953) and of Bowles–MacKenzie (1954) and the prism-matching theory of Bilby–Frank (1960). A macroscopic shear of 0·078 is predicted by the phenomenological theory of W.–L.–R., while the minimum shape deformation criterion of Bilby–Frank predicts a macroscopic shear of 0·07.

The transformation from the UC_2 cubic to UC_2 tetragonal lattice can be easily visualized if the tetragonal lattice is reindexed by a 45° rotation along the c axis so that $c' = c$ and $a' = a/2$. The transformation from the UC_2 cubic lattice ($a_0 \cong 5{\cdot}41$ Å at 1820 °C.) to the reindexed UC_2 tetragonal lattice ($a' \cong 5{\cdot}20$, $c' \cong 5{\cdot}88$ Å at 1820 °C.) is then very similar to that of ZrH_2 or TiH_2.

The shear mechanism suggests possibly that the high temperature structure of UC_2 still contains the discrete C_2 groups of the low temperature form. This appears interesting in view of the supposed miscibility of UC and UC_2 above about 1900 °C. (Rough & Bauer, 1958). However, our recent high temperature X-ray diffraction data (unpublished) confirm the co-existence of two cubic UC and UC_2 phases near 2000 °C. Unfortunately, the diffraction patterns obtained at temperatures much above 2000 °C. are inconclusive to tell whether the two cubic phases still co-exist. Chubb & Phillips recently proposed an entirely different phase diagram imposing the complete immiscibility of UC and UC_2 up to the melting temperature based on metallographic evidence of quenched samples (Chubb & Phillips). Furthermore, the shear type transformation does not exclude a possible local rearrangement of the C atoms to permit the formation of C_2 groups during transformation to the low temperature phase. It appears, therefore, desirable to redetermine the crystal structure of the high temperature UC_2 phase by means of X-ray and neutron diffraction. The exact positions of the C atoms in the high tem-

* This work was supported by the U.S. Atomic Energy Commission.

† The true crystal structure of the high temperature UC_2 cubic phase is not yet certain. It is quoted by several investigators (see Rough & Bauer, 1958, and Austin, 1959) to have the CaF_2 structure.

perature UC_2 phase may throw further light on the UC–UC_2 miscibility problem.

References

AUSTIN, A. E. (1959). *Acta Cryst.* **12**, 159.

BILBY, B. A. & FRANK, F. C. (1960). *Acta Met.* **8**, 239.

BOWLES, J. S. & MACKENZIE, J. K. (1954). *Acta Met.* **2**, 129, 224.

CHANG, R. (1960). *J. Nuclear Materials*, **2**, 335.

CHUBB, W. & PHILLIPS, W. M. *Battelle Memorial Institute Report.* To be published.

ROUGH, F. A. & BAUER, A. A. (1958). *Constitutional Diagrams of Uranium and Thorium Alloys*, Addison-Wesley.

WESCHLER, M. S., LIEBERMAN, D. S. & READ, T. A. (1953). *Trans. Amer. Inst. Min. (Metall.) Engrs.* **197**, 1503.

WILSON, W. B. (1960). *J. Amer. Ceram. Soc.* **43**, 77.

YAKEL, JR. H. L. (1958). *Acta Cryst.* **11**, 46.

Acta Cryst. (1961). **14**, 1098

Transitional cryptoperthites.

By A. B. MUKHERJEE, *Department of Geology and Geophysics, Indian Institute of Technology, Kharagpur, West Bengal, India*

(*Received* 22 *March* 1961)

In course of a study of some photometrically analyzed cryptoperthites and X-ray perthites of the Malani rhyolites of W. Rajasthan, reciprocal lattice angles α^* and γ^* of the unmixed sodarich phases have been determined from the albite- and pericline-twinned individuals using the *b*-axis X-ray oscillation method of Smith & Mackenzie (1955).

Table 1 gives the chemical composition and optic axial angles together with the reciprocal lattice angles α^* and γ^* of the unmixed phases (where they could be measured). To compare these values with those of the natural alkali feldspars of different composition and from different geological environments the values of α^* of the unmixed soda-rich phases have been plotted against the corresponding values of γ^* (after Mackenzie & Smith, 1955). Each plot has been indexed for correlation with Table 1. In Fig. 1 have also been plotted α^* and γ^* of orthoclase (monoclinic potash feldspar), maximum microcline (Mackenzie, 1956); two intermediate microclines; high-temperature albite and synthetic feldspars $Or_{10}Ab_{90}$, $Or_{20}Ab_{80}$, $Or_{30}Ab_{70}$ and low-temperature albite. Apart from these plots for reference, corresponding positions for the sanidine cryptoperthites and orthoclase microperthites studied by Mackenzie & Smith (Figs. 2 and 3 in Mackenzie & Smith, 1956) are shown by symbols (Fig. 1).

In this diagram positions of the α^*–γ^* plots of the rhyolitic alkali feldspars from Rajasthan show that most of these unmixed feldspars have soda phases which are possibly transitional between the high- and low-temperature modifications of the soda-rich alkali feldspars. This possibility is indicated by optic axial measurements also. The values of the optic angles (Table 1) have been plotted on a slightly modified form of Tuttle's (1952) diagram which shows the relation between optic angle and chemical composition in the alkali feldspar series. It will be seen from the position of the plots in the diagram (Fig. 2) that the examined feldspars have optic axial angles roughly intermediate between those of sanidine–cryptoperthites and orthoclase–microperthites within the same compositional range.

Mackenzie & Smith (1955, 1956) have found that the soda-rich phase of the orthoclase microperthites and sanidine cryptoperthites have reciprocal lattice angles α^* and γ^* close to those of low-temperature and high-temperature soda-rich feldspars respectively. Tuttle & Keith (1954) have shown that specimens which optically fall intermediate between the orthoclase microperthite

Table 1

		Composition			Reciprocal lattice angles: Na-phase (Albite twinned)		K-phase	
Sp. no.	Plot no.	Or.	(Ab + An)	$2V_\alpha$	α^*	γ^*	α^*	γ^*
*M*581	1	60·2	39·8	80–82·5	88° 1′	89° 52′		
*M*586	2	60·8	39·2	79·2–83·1	88° 7′	90°		
*M*562	3	64·2	35·8	48·4	88° 27′	90°		
*M*2393	4	50·6	49·4	60·5–66·0	87° 38′	90°		
*M*2389	5	42·3	57·7	80·2–84·3	86° 40′	89° 50′		
*M*1808	6	54·2	45·8	62·5–65·0	87° 45′	89° 44′		
*M*2103	7	59·5	40·5		87° 54′	90°	90° 49′	90° 52
*M*301	8	59·8	40·2	74·5–77·2	87° 57′	89° 50′		
*M*2437	9				87° 54′	90°	90° 45′	91° 5′
*M*2225	10	60·1	39·9	81·1	88° 1′	90°		
*M*1849	11	62·7	37·3		88° 1′	90°		
*M*2307	12	59·6	40·4		88° 3′	90°	91° 3′	90° 9′
*M*1535	13	49·3	50·7	76·5–82·3	87° 48′	90°		
*M*2147	14				87° 38′	90°	91° 34′	90° 10′
*M*308	15				87° 22′	89° 42′		